Med Chem Res
DOI 10.1007/s00044-017-1867-0

MEDICINAL CHEMISTRY RESEARCH

ORIGINAL RESEARCH

Structure-based design, synthesis, PPAR-γ activation, and molecular docking of *N*-substituted phthalimides

Bin Xiao[1] · **Shumin Wang**[1] · **Zhanfei She**[1] · **Qingfeng Cao**[1] · **Na Zhao**[1] · **Xiangrong Tian**[2] · **Yixin Su**[1]

Received: 12 October 2015 / Accepted: 4 March 2017

Abstract *N*-substituted phthalimides showed peroxisome proliferator-activated receptors-γ activation in rat liver epithelial Ac2F cells in our previous study. In order to explore better peroxisome proliferator-activated receptors-γ agonists, new *N*-substituted phthalimide derivatives were designed and synthesized based on a pharmacophore study of natural peroxisome proliferator-activated receptors-γ agonist paecilocin A and synthetic leads. Peroxisome proliferator-activated receptors-γ activation by the new derivatives was evaluated using rat liver epithelial Ac2F cells at a concentration of 10 μM (same as previous study). All the new derivatives showed comparable or better activities than that of rosiglitazone, in which 3-hydroxy-*N*-(*p*-methoxy-phenethyl) phthalimide (compound **6**) appeared as the best. Molecular docking suggested that the free hydroxyl group on the phthalimide head, a proper hydrophobic tail including a phenyl linker, were beneficial for peroxisome proliferator-activated receptors-γ activation. These *N*-substituted phthalimide derivatives are valuable as scaffolds for new peroxisome proliferator-activated receptors-γ agonists.

Keywords PPAR-γ · Diabetes · Phthalimide · Luciferase assay · Docking simulation

Introduction

Peroxisome proliferator-activated receptors (PPARs) belong to the nuclear receptor superfamily of ligand-activated transcription factors, and comprise three members: PPAR-α, β/δ, and γ (Mangelsdorf et al. 1995; Nuclear Preceptors Nomenclature Committee 1999; Berger and Moller 2002; Evans et al. 2004). PPAR-γ is predominantly expressed in adipose tissue, colon, and macrophages, and play an important role in the regulation of insulin sensitivity, fatty acid storage, adipogenesis, and glucose metabolism (Spiegelman 1998). Although PPAR-γ agonists such as thiazolidinediones (TZDs, e.g., rosiglitazone (Ros) and troglitazone) are used to treat type II diabetes mellitus, the adverse effects including an increased risk of heart attack, weight gain, edema, and fluid retention remain challenges. New PPAR-γ ligands with less adverse effects are still in demand for treatment of type II diabetes mellitus (Willson et al. 2000).

A ternary complex structure (2PRG) composed of the PPAR-γ ligand-binding domain (LBD), Ros, and human steroid receptor co-activating factor-1 was reported, and we summarized the key pharmacophore concept of Ros (Fig. 1a) (Nolte et al. 1998; Xiao et al. 2012). In our previous study, based on a pharmacophore study of paecilocin A (a natural PPAR-γ agonist paecilocin A, Fig. 2a) and synthetic PPAR-γ agonists (TZDs and Tyrosine derivatives, Fig. 2a), we proposed that the 3-hydrophthalic moiety of paecilocin A function as a hydrophilic head and form

Electronic supplementary material The online version of this article (doi:10.1007/s00044-017-1867-0) contains supplementary material, which is available to authorized users.

✉ Yixin Su
suyixin8888@163.com

[1] Ordos School of Clinical Medicine, Inner Mongolia Medical University, Ordos 017000, China

[2] College of Plant Protection, Northwest A&F University, Yangling 712100, China

Published online: 28 March 2017

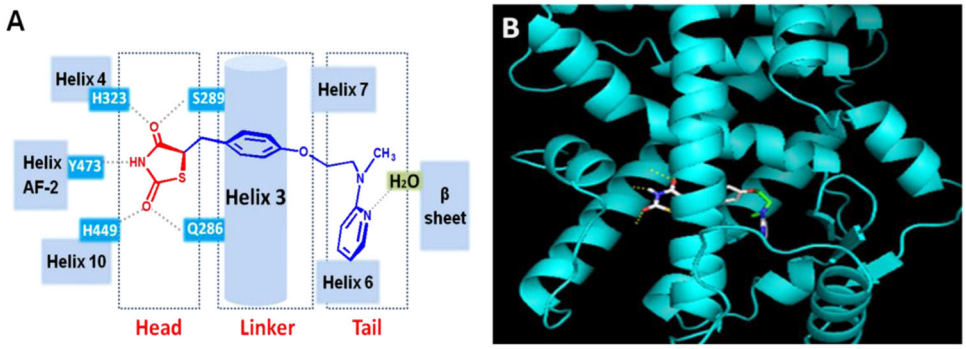

Fig. 1 **a** Graphical illustration of the key pharmacophore concept of Ros. The Ros skeleton was considered a combination of a head, linker, and tail. Carbonyl oxygen and nitrogen in the head form hydrogen bonds with residues H^{323}, S^{289}, H^{449}, Q^{286}, and Y^{473}, which are crucial for PPAR-γ activation; central aromatic ring and oxygen occupied a hydrophobic pocket behind Helix 3 as a linker; tail group occupied a larger pocket between Helix 3 and β-sheet, in which the nitrogen forms a key hydrogen bond with water molecule H_2O^{604}. **b** Superposition of hPPAR-γ LBD binding with Ros (docking simulation). The protein is represented as a cartoon (*cyan*) and Ros as sticks (*purple*) (color figure online)

H-bonds with key amino acid residues of PPAR-γ LBD: Tyr^{473}, His^{449}, His^{323}, and Ser^{289} (Xiao et al. 2012).

The easily accessible phthalimide moiety has often been employed as a pharmacophore in drug development (Pessoa et al. 2010; Motoshima et al. 2011). In our further study, phthalimide-derived molecules were designed (Fig. 2b), produced, and evaluated with respect to PPAR-γ activation in rat liver Ac2F cells, and these phthalimide derivatives were investigated as a new class of PPAR-γ ligands (Xiao et al. 2014). Previously we had studied the dose-dependent activity of the *N*-substituted phthalimide skeleton (Xiao et al. 2012; Xiao et al. 2014), in the present study, further derivation of *N*-substituted phthalimide was performed and PPAR-γ activation by the new derivatives was evaluated using rat liver epithelial Ac2F cells at a concentration of 10 μM.

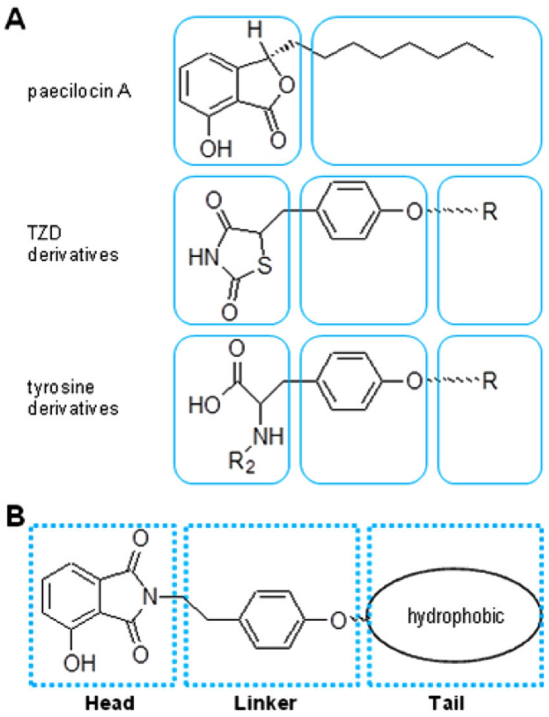

Fig. 2 **a** Simplified topology of paecilocin A and of typical synthetic PPAR-γ agonists. Paecilocin A contains a hydrophilic 3-hydroxy phthalide moiety and a hydrophobic octyl chain; both TZD and tyrosine derivatives employ a phenol moiety as linker, connecting a hydrophilic head and a hydrophobic tail. **b** Molecular design of the *N*-substituted phthalimide skeleton of PPAR-γ agonists; a 3-hydroxy phthalimide moiety acts as the head, a phenol moiety as the central linker, a hydrophobic substituent acts as the tail

Material and methods

General

^1H and ^{13}C NMR spectra were recorded on a Varian Unity 400 MHz NMR spectrometer, and chemical shifts are reported with respect to respective residual solvent or deuterated solvent peaks (δ_H 3.30 and δ_C 49.0 for CD_3OD, δ_H 7.24 and δ_C 76.8 for $CDCl_3$). FAB MS data was obtained using a JEOL JMS SX-102A spectrometer. High performance liquid chromatography (HPLC) was performed using a YMC ODS-H80 column (250 × 10 mm, 4 μm, 80 Å) or a C18-5E Shodex packed column (250 × 10 mm, 5 μm, 100 Å) and a Shodex RI-71 detector.

General synthetic methods for compounds **1–7** are shown in Scheme 1. Unless otherwise noted, reagents and solvents used were from commercial source. All synthesized compounds were purified to be 99% pure by a RP-HPLC using 90% aqueous MeCN as eluent.

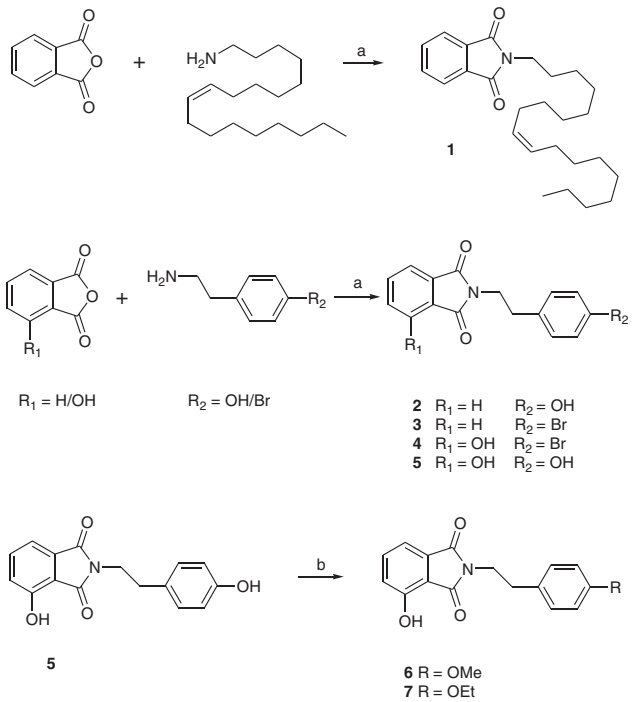

Scheme 1 Synthesis of phthalimide derivatives (**1–7**). Reagents and conditions: **a** CH_3COOH, 85 °C, overnight; **b** RI, Ag_2O, stir, CH_3CN, reflux for 12 h

*General procedure for the synthesis of the compounds **1–5***

A mixture of amine (1.2 equiv) and phthalic anhydride in aqueous glacial acetic acid (1 M) was stirred and heated under reflux overnight. Products was precipitated by adding water, filtered, and washed thoroughly with water. Residues were diluted with MeOH, dried with $MgSO_4$, and evaporated to provide the crude products **1–5** (yield ~90%).

N-Oleyl phthalimide (**1**) White powder; ^{1}H NMR ($CDCl_3$, 400 MHz): δ 0.85 (t, $J = 7.2$ Hz, 3H, CH_3), 1.20 (m, 22H, CH_2), 1.63 (m, 2H,=N–CH_2–CH_2–), 1.98 (m, 4H,=CH–CH_2–), 3.60 (t, $J = 7.6$ Hz, 2H,=N–CH_2–CH_2–), 5.30 (m, 2H,=CH–), 7.78 (m, 4H, Ar); ^{13}C NMR ($CDCl_3$, 100 MHz): δ 168.7 (C, C=O), 134.0 (C, C-3a, 7a), 132.4 (C, C-5, 6), 132.3 (C, C-9′, 10′), 123.3 (C, C-4, 7), 38.3 (C, C-1′), 32.8 (C, C-16′), 32.1 (C, C-14′), 30.0 (C, C-6′), 29.9 (C, C-13′), 29.9 (C, C-5′), 29.7 (C, C-12′), 29.6 (C, C-7′), 29.5 (C, C-4′), 29.4 (C, C-15′), 28.8 (C, C-2′), 27.4 (C, C-8′), 27.4 (C, C-11′), 27.1 (C, C-3′), 22.9 (C, C-17′), 14.3 (C, C-18′); FABMS *m/z* 398 $[M + H]^+$.

N-(p-Hydroxy-phenethyl) phthalimide (**2**) White powder; ^{1}H NMR (CD_3OD, 400 MHz): δ 2.84 (t, $J = 7.2$ Hz, 2H, phen–CH_2–CH_2–), 3.81 (t, $J = 7.6$ Hz, 2H, phen–CH_2–CH_2–), 6.62 (d, $J = 8.4$ Hz, 2H, H–ortho phenol), 6.98 (d, $J = 8.4$ Hz, 2H, H–meta phenol), 7.77 (m, 4H, Ar); ^{13}C NMR (CD_3OD, 100 MHz): δ 168.5 (C, C=O), 155.9 (C, C–OH), 134.1 (C, C–para phenol), 132.1 (C, C-3a), 129.6 (C, C-5), 129.0 (C, C-4), 122.8 (C, C–meta phenol), 115.1 (C, C–ortho phenol), 39.4 (C, phen–CH_2–CH_2–), 33.2 (C, phen–CH_2–CH_2–); FABMS *m/z* 268 $[M + H]^+$.

N-(p-Bromo-phenethyl) phthalimide (**3**) White powder; ^{1}H NMR ($CDCl_3$, 400 MHz): δ 2.93 (t, $J = 7.2$ Hz, 2H, phen–CH_2–CH_2–), 3.87 (t, $J = 7.6$ Hz, 2H, phen–CH_2–CH_2–), 7.11 (d, $J = 8.4$ Hz, 2H, H–ortho phen–Br), 7.36 (d, $J = 8.4$ Hz, 2H, H–meta phen–Br), 7.78 (m, 4H, Ar); ^{13}C NMR ($CDCl_3$, 100 MHz): δ 168.3 (C, C=O), 137.1 (C, C–para phen–Br), 134.2 (C, C-3a), 132.2 (C, C-5), 131.8 (C, C–ortho phen–Br), 130.8 (C, C–meta phen–Br), 123.5 (C, C-4), 120.8 (C, C–Br), 39.1 (C, phen–CH_2–CH_2–), 34.2 (C, phen–CH_2–CH_2–); FABMS *m/z* 330 $[M + H]^+$.

3-Hydroxy-N-(p-bromo-phenethyl) phthalimide (**4**) White powder; ^{1}H NMR ($CDCl_3$, 400 MHz): δ 2.92 (t, $J = 7.6$ Hz, 2H, phen–CH_2–CH_2–), 3.84 (m, 2H, phen–CH_2–CH_2–), 7.09 (d, $J = 8.4$ Hz, 2H, H–meta phen–Br), 7.13 (d, $J = 8.8$ Hz, 1H, H-4), 7.34 (d, $J = 7.2$ Hz, 1H, H-6), 7.38 (d, $J = 8.4$ Hz, 2H, H–ortho phen–Br), 7.55 (t, $J = 7.6$ Hz, 1H, H-5), 7.57 (s, 1H, OH); ^{13}C NMR ($CDCl_3$, 100 MHz): δ 170.3 (C, β–C=O, –OH), 167.9 (C, γ–C=O, –OH), 154.9 (C, C–OH), 137.0 (C, C–para phen–Br), 136.6 (C, C-6a), 132.2 (C, C-5), 131.9 (C, C–ortho phen–Br), 130.7 (C, C–meta phen–Br), 122.9 (C, C–Br), 120.9 (C, C-6), 116.2 (C, C-3a), 114.7 (C, C-4), 39.0 (C, phen–CH_2–CH_2–), 34.2 (C, phen–CH_2–CH_2–); FABMS *m/z* 346 $[M + H]^+$.

3-Hydroxy-N-(p-hydroxy-phenethyl) phthalimide (**5**) White powder; ^{1}H NMR (CD_3OD, 400 MHz): δ 2.81 (t, $J = 7.2$ Hz, 2H, phen–CH_2–CH_2–), 3.74 (t, $J = 7.6$ Hz, 2H, phen–CH_2–CH_2–), 6.63 (d, $J = 8.4$ Hz, 2H, H–ortho HO–phenethyl), 6.98 (d, $J = 8.4$ Hz, 2H, H–meta HO–phenethyl), 7.09 (d, $J = 8.0$ Hz, 1H, H-4), 7.27 (d, $J = 7.2$ Hz, 1H, H-5), 7.52 (t, $J = 7.6$ Hz, 1H, H-6); ^{13}C NMR (CD_3OD, 100 MHz): δ 168.4 (C, β–C=O, –OH), 168.1 (C, γ–C=O, –OH), 155.9 (C, C-3), 155.2 (C, C–OH phenethyl), 135.8 (C, C-6a), 133.6 (C, C-5), 129.6 (C, C–para HO–phenethyl), 129.2 (C, C–meta HO–phenethyl), 122.9 (C, C-6), 115.1 (C, C-3a), 115.0 (C, C-4), 114.4 (C, C–ortho HO–phenethyl), 39.1 (C, phen–CH_2–CH_2–), 33.3 (C, phen–CH_2–CH_2–); FABMS *m/z* 284 $[M + H]^+$.

*General procedure for the synthesis of the compounds **6–7***

To a solution of 3-hydroxy-*N*-(*p*-hydroxy-phenethyl) phthalimide **5** (13 mg, 0.046 mmol) in CH_3CN (1.5 ml), RI (CH_3I: 6.0 µl, ca. 0.09 mmol; CH_3CH_2I: 7.0 µl, ca. 0.09 mmol) and Ag_2O (10 mg, 0.04 mmol) were added. The mixture was then heated under reflux with stirring for 12 h.

Solid material was removed by filtration, solvent was removed by evaporation, and the solid material obtained was purified by RP HPLC using 90% aqueous MeOH as eluant to give **6–7** (yield ~75%).

3-Hydroxy-N-(p-methoxy-phenethyl) phthalimide (**6**) White powder; ^{1}H NMR (CD_3OD, 400 MHz): δ 2.82 (t, $J = 7.6$ Hz, 2H, phen–C<u>H</u>$_2$–CH_2–), 3.76 (m, 2H, phen–CH_2–C<u>H</u>$_2$–), 3.96, (s, 3H, OMe), 6.63 (d, $J = 8.4$ Hz, 2H, H–ortho HO–phenethyl), 6.98 (d, $J = 8.8$ Hz, 2H, H–meta HO–phenethyl), 7.35 (d, $J = 7.2$ Hz, 1H, H-4), 7.36 (d, $J = 8.8$ Hz, 1H, H-5), 7.70 (t, $J = 7.6$ Hz, 1H, H-6); ^{13}C NMR ($CDCl_3$, 100 MHz): δ 168.1 (C, β–C=O, –OH), 167.2 (C, γ–C=O, –OH), 156.8 (C, C–OMe), 154.4 (C, C–OH), 136.3 (C, C-6a), 136.3 (C, C-5), 134.4 (C, C–para –OMe), 130.5 (C, C–meta –OMe), 130.2 (C, C-6), 117.6 (C, C-3a), 115.7 (C, C-4), 115.6 (C, C–ortho –OMe), 56.5 (C, –OMe), 39.5 (C, phen–CH_2–C<u>H</u>$_2$–), 33.8 (C, phen–C<u>H</u>$_2$–CH_2–); FABMS *m/z* 298 $[M + H]^+$.

3-Hydroxy-N-(p-ethoxy-phenethyl) phthalimide (**7**) White powder; ^{1}H NMR (CD_3OD, 400 MHz): δ 1.44 (t, $J = 7.2$ Hz, 3H, O–CH_2C<u>H</u>$_3$), 2.82 (t, $J = 7.6$ Hz, 2H, phen–C<u>H</u>$_2$–CH_2–), 3.76 (m, 2H, phen–CH_2–C<u>H</u>$_2$–), 4.24 (q, $J = 6.8$, 7.2 Hz, 2H, O–C<u>H</u>$_2$$CH_3$), 6.63 (d, $J = 8.4$ Hz, 2H, H–ortho –OEt), 6.98 (d, $J = 8.8$ Hz, 2H, H–meta –OEt), 7.33 (d, $J = 7.2$ Hz, 1H, H-4), 7.34 (d, $J = 8.8$ Hz, 1H, H-5), 7.67 (t, $J = 7.6$ Hz, 1H, H-6); ^{13}C NMR ($CDCl_3$, 100 MHz): δ 168.2 (C, β–C=O, –OH), 167.2 (C, γ–C=O, –OH), 156.8 (C, C–OEt), 154.4 (C, C–OH), 136.2 (C, C-6a), 136.2 (C, C-5), 134.5 (C, C–para –OEt), 130.4 (C, C–meta –OEt), 130.2 (C, C-6), 118.7 (C, C-3a), 115.6 (C, C-4), 115.5 (C, C–ortho –OMe), 65.2 (C, –O–C<u>H</u>$_2$–CH_3), 39.5 (C, phen–CH_2–C<u>H</u>$_2$–), 33.9 (C, phen–C<u>H</u>$_2$–CH_2–), 14.8 (C, –O–CH_2–C<u>H</u>$_3$); FABMS *m/z* 312 $[M + H]^+$.

Biological assay

For luciferase assays, plasmids were transfected into Ac2F cells in a 48-well plate (5 × 104 cells/well) with effector plasmids and the TK-PPRE × 3-luciferase reporter plasmid (1 μg/well) plus pcDNA3(0.1 μg/well) or pFlag-PPAR-γ1 (0.1 μg/well) using Lipofectamine™ 2000 (Invitrogen Co., USA), according to the manufacturer's instructions. After transfection for 4 h, conditioned media was replaced with complete medium, and cells were incubated for an additional 20 h. The medium was then removed, and cells were exposed in serum-free media to Ros or test compounds for 6 h, washed with PBS and assayed using the ONE-Glo™ Luciferase Assay System (Promega, Madison, WI, USA). Luciferase activities were measured using a GloMax®-Multi Microplate Multimode Reader (Promega Co., Sunny Vale, CA, USA). ANOVA was used to determine the significances of differences between groups, whereas differences between the mean of individual groups were assessed using Fisher's protected LSD post hoc test. *P* values of <0.05 were considered statistically significant.

Molecular docking

Protein coordinates were downloaded from the Protein Data Bank (accession code: 2PRG) (Berman et al. 2000). Chain A was prepared for docking within the molecular modeling software package Chimera 1.5.3 (National Institutes of Health, Bethesda, MD, USA) (Pettersen et al. 2004). Polar hydrogen and setting grid box parameters were added using MGLTools 1.5.4 (The Scripps Research Institute, La Jolla, CA, USA) (Michel and Sanner 1999; Morris et al. 2009). Docking calculations were performed using AutoDock Vina 1.1.2 software (The Scripps Research Institute, La Jolla, CA, USA) (Trott and Olson 2010). Default settings and the Vina scoring function were applied. For ligand preparation, Chem3D Ultra 8.0 software (CambridgeSoft Corporation, Cambridge, MA, USA) was used to convert the 2D structures of candidates into 3D structural data. The analysis and visual investigation of ligand-protein interactions of docking poses were performed using PyMol v1.7.4 (The PyMOL Molecular Graphics System, Schrodinger LLC, New York, NY, USA).

For validation of docking simulation, Ros was re-docked into 2PRG complex. Chain A, chain B, and several important water molecules were tested for generating top-ranked and reproducible binding modes that are close to those of the 2PRG crystal, finally chain A and H_2O^{308}, H_2O^{339}, H_2O^{444}, and H_2O^{467} were selected for PPAR-γ agonist docking workflow, and a search grid box was set to

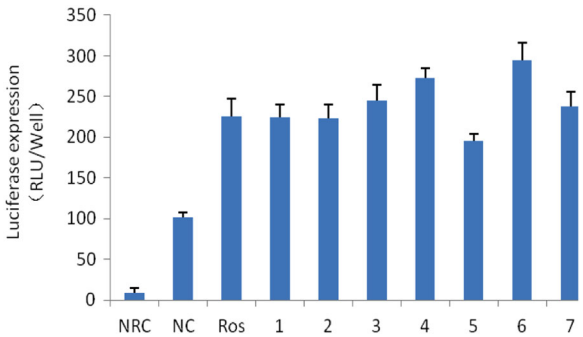

Fig. 3 In vitro assay of PPAR-γ activation by phthalimides **1–7** and by Ros at a concentration of 10 μM in rat liver epithelial Ac2F cells. No receptor control (without plasmid transfection), negative control (transfected with a plasmid containing PPRE and pcDNA), Ros. Ros was used as positive control to monitor luciferase activations. Compound-treated cells were transiently transfected with PPRE plus pFlag-PPAR-γ1. Luciferase expressions (relative light units (RLU)/well) are the means + SDs of five independent results.

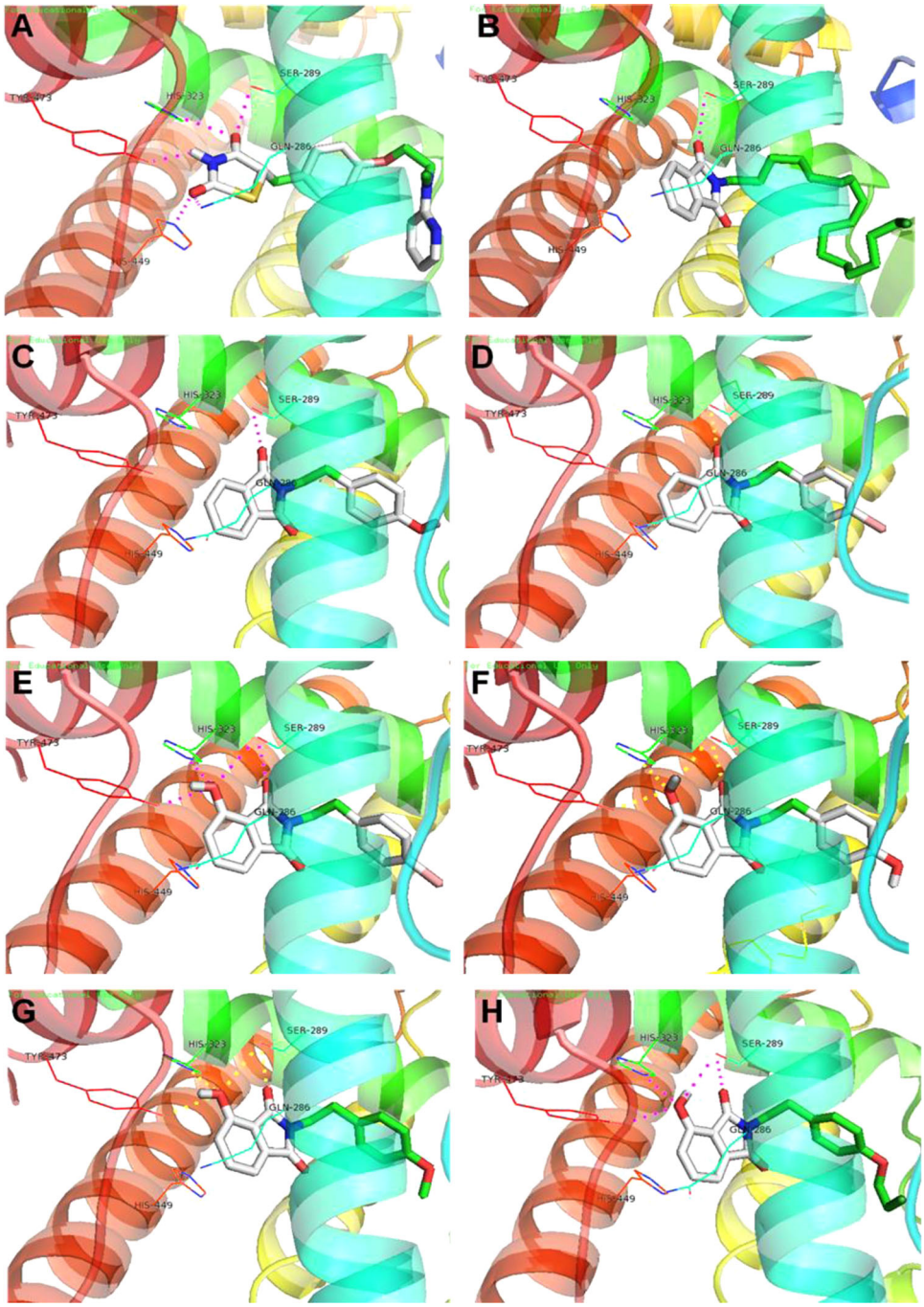

Fig. 4 The 3D putative binding modes of Ros and **1–7** with PPAR-γ LBD. The key amino acid residues including Tyr^{473}, His^{449}, His^{343}, Ser^{289}, and Glu^{286} were labeled and the formed H bonds were shown in the pictures. **a** Ros interacts with key amino acid residues (Tyr^{473}, His^{449}, His^{343}, Ser^{289}, and Glu^{286}) in the PPAR-γ binding pocket (−8.2 kcal/mol); **b** Binding mode of **1** (−6.3 kcal/mol); **c** Binding mode of **2** (−7.6 kcal/mol); **d** Binding mode of **3** (−7.8 kcal/mol); **e** Binding mode of **4** (−8.3 kcal/mol); **f** Binding mode of **5** (−8.4 kcal/mol); **g** Binding mode of **6** (−8.5 kcal/mol); **h** Binding mode of **7** (−8.6 kcal/mol)

cover the whole surface of the protein to collect all possible orientations and conformations of the ligand paired with the protein. Synthesized compounds were compared with Ros in four aspects; affinity of the top-ranked mode (AT), average affinity of the nine generated modes (AM), the number of modes located in the binding pocket (NM), the average number of H-bond interactions with key amino acid residues (AI).

Results and discussion

Synthesis

N-substituted phthalimides can be prepared by heating phthalic anhydride with various *N*-containing reagents (Pluempanupat et al. 2007). Compounds **1–5** were generated by heating phthalic anhydride or 3-hydroxyphthalic

anhydride with oleyl, *p*-hydroxy-phenethyl or *p*-bromo-phenethyl amine in the presence of acetic acid to afford a 90% yield. Compound **1** was to imitate the skeleton of lipidic PPAR-γ agonists and paecilocin A (Fig. 2a), while compounds **2–5** were to imitate the topology of synthetic PPAR-γ agonists (e.g., Ros, farglitazar). Short alkyl chains methyl and ethyl were added to the phenyl moiety by etherification, and the major products obtained were monoalkylated on the phenol group (**6–7**) at a yield around 75%. All of their structures were characterized.

PPAR-γ activation

Synthesized compounds were subsequently evaluated for PPAR-γ activation in rat liver epithelial Ac2F cells transiently transfected with pcDNA3 + PPRE or pFlag-PPAR-γ1 + PPRE. As shown in Fig. 3, all compounds showed PPAR-γ activation at the concentration of 10 μM, the potencies of compounds **1** and **2** were comparable to that of rosiglitazone, while compounds **3**, **4**, **6**, and **7** showed greater potencies than that of Ros, and compound **5** showed moderate potency. Etherization of compound **5** (**6** and **7**) while keeping a free hydroxyl group on the phthalimide moiety significantly improved the PPAR-γ activation of compound **5**. Compound **6**, which has a methyl tail, exhibited most potent activity.

Different Log *P* values of synthetic analogues could have led to cell permeability differences in Ac2F cells (Kubinyi 1979; Lipinski et al. 2001). Furthermore, the mechanism of PPAR-γ activation is complicated and different ligands are likely to alter the conformation of PPAR-γ protein in different way, which could affect co-activator recruitment (Itoh et al. 2008; Waku et al. 2009; Waku et al. 2010; Porcelli et al. 2012). Other factors might also modulate the bioavailabilities of these molecules in vivo. Therefore, further intensive optimization and in vivo evaluations of these molecules is required.

Molecular docking and SAR

According to docking simulation, these compounds bind to PPAR-γ LBD in the same manner as Ros (Fig. 4). Binding affinities of compounds **1–3** were lower than Ros while that of **4–7** were higher than Ros (Table 1), however, compounds **1–3** showed comparable PPAR-γ activation to that of Ros might because the relatively high Log *P* values of compounds **1–3** led to good cell permeability, in which compound **3** with relatively higher binding affinity but lower Log *P* value appeared better than **1** and **2**. The 3-hydroxy-phthalimide head of compounds **4–7** formed several hydrogen bonds with key amino acid residues (especially Tyr^{473} on helix 12) of PPAR-γ LBD (Fig. 4e–h),

Table 1 Docking analysis results for compounds **1–7** and Ros

Compounds	AT[a]	AM[b]	NM[c]	AI[d]	Log *P*
1	−6.3	−6.178	2	0.00	9.54 ± 0.36
2	−7.6	−7.144	5	0.40	4.52 ± 0.36
3	−7.8	−7.300	8	1.00	3.01 ± 0.26
4	−8.3	−7.189	3	1.67	3.78 ± 0.79
5	−8.4	−7.356	4	1.75	2.28 ± 0.75
6	−8.5	−7.400	4	2.00	2.93 ± 0.75
7	−8.6	−7.356	6	1.17	3.46 ± 0.75
Ros	−8.2	−7.033	4	1.50	2.56 ± 0.79

[a] AT, affinity of the top-ranked mode

[b] AM, average affinity of the nine generated modes

[c] NM, the number of modes located in the binding pocket

[d] AI, the average number of H-bond interactions with key amino acid residues

this H-bond network might stabilize PPAR-γ in the conformation required for successful co-activator recruitment and PPAR-γ activation (Nolte et al. 1998; Kuhn et al. 2006). According to Linpinski's Rule of 5, compound **1** with high Log *P* value is less druggable. Log *P* value of compound **5** is lower than Ros, moderate cell permeability might lead to its moderate cell-based PPAR-γ activation.

Compared with **5**, methylated (**6**) and ethylated (**7**) derivatives significantly increased PPAR-γ activation. Previous studies have shown that a hydrophobic substituent provides a good tail for PPAR-γ agonists (Santini et al. 2003). Here, we confirmed that connecting the phenoxyl moiety with a hydrophobic tail designed to occupy the hydrophobic binding pocket in PPAR-γ LBD enhanced binding between 3-hydroxy-*N*-phenethyl phthalimide (**5**) and PPAR-γ LBD. Methyl group activated PPAR-γ better than ethyl group, Log *P* values of synthetic analogues (**6** and **7**) and other factors could have led to PPAR-γ activation differences in Ac2F cells.

Conclusion

In conclusion, we synthesized a new group of *N*-substituted phthalimides based on the results of a pharmacophore study of natural (paecilocin A) and synthetic PPAR-γ agonists as well as our previous study. The incorporation of proper hydrophilic and hydrophobic groups into a phthalimide skeleton yielded novel PPAR-γ agonists, which showed cell-based activities comparable to that of Ros. A free hydroxyl group on the phthalimide moiety and hydrophobic tail groups (especially the methoxyl group) were found to be beneficial for PPAR-γ activation. These *N*-substituted phthalimide derivatives are valuable as scaffolds for new

PPAR-γ agonists, further optimization and in vivo evaluation of these molecules would provide valuable data.

Compliance with ethical standards

Conflicts of Interest The authors declare that they have no competing interests.

References

Berger J, Moller DE (2002) The mechanisms of action of PPARs. Annu Rev Med 53:409–435

Berman HM, Westbrook J, Feng Z, Gilliland G, Bhat TN, Weissig H, Shindyalov IN, Bourne PE (2000) The protein data bank. Nucl Acids Res 28:235–242

Evans RM, Barish GD, Wang YX (2004) PPARs and the complex journey to obesity. Nat Med 10:355–361

Itoh T, Fairall L, Amin K, Inaba Y, Szanto A, Balint BL, Nagy L, Yamamoto K, Schwabe JWR (2008) Structural basis for the activation of PPARγ by oxidized fatty acids. Nat Struct Mol Biol 15:924–931

Kubinyi H (1979) Nonlinear dependence of biological activity on hydrophobic character: the bilinear model. Farmaco Sci 34:248–276

Kuhn B, Hilpert H, Benz J, Binggeli A, Grether U, Humm R, Märki HP, Meyer M, Mohr P (2006) Structure-based design of indole propionic acids as novel PPARalpha/gamma co-agonists. Bioorg Med Chem Lett 16:4016–4020

Lipinski CA, Lombardo F, Dominy BW, Feeney PJ (2001) Experimental and computational approaches to estimate solubility and permeability in drug discovery and development settings. Adv Drug Deliv Rev 46:3–26

Mangelsdorf DJ, Thummel C, Beato M, Herrlich P, Schötz G, Umesono K, Blumberg B, Kastner P, Mark M, Chambon P (1995) The nuclear receptor superfamily: the second decade. Cell 83:835–839

Michel F, Sanner (1999) Python: a programming language for software integration and development. J Mol Graphics Mod 17:57–61

Morris GM, Huey R, Lindstrom W, Sanner MF, Belew RK, Goodsell DS, Olson AJ (2009) Autodock4 and AutoDockTools4: automated docking with selective receptor flexiblity. J Comput Chem 16:2785–2791

Motoshima K, Ishikawa M, Hashimoto Y, Sugita K (2011) Peroxisome proliferator-activated receptor agonists with phenethylphenylphthalimide skeleton derived from thalidomide-related liver X receptor antagonists. Bioorg Med Chem 19:3156–3172

Nolte RT, Wisely GB, Westin S, Cobb JE, Lambert MH, Kurokawa R, Rosenfeld MG, Willson TM, Glass CK, Milburn MV (1998) Ligand binding and co-activator assembly of the peroxisome proliferator-activated receptor-gamma. Nature 395:137–143

Nuclear Receptors Nomenclature Committee (1999) A unified nomenclature system for the nuclear receptor superfamily. Cell 97:161–163

Pessoa C, Ferreira PMP, Lotufo LV, Moraes MO, Cavalcanti SMT, Coêlho LCD, Hernandes MZ, Leite ACL, DeSimone CA, Costa VMA (2010) Discovery of phthalimides as immunomodulatory and antitumor drug prototypes. Chem Med Chem 5:523–528

Pettersen EF, Goddard TD, Huang CC, Couch GS, Greenblatt DM, Meng EC, Ferrin TE (2004) UCSF Chimera-a visualization system for exploratory research and analysis. J Comput Chem 13:1605–1612

Pluempanupat W, Adisakwattana S, Yibchok-Anun S, Chavasiri W (2007) Synthesis of N-phenylphthalimide derivatives as alpha-glucosidase inhibitors. Arch Pharm Res 30:1501–1506

Porcelli L, Gilardi L, Laghezza A, Piemontese L, Mitro N, Azzariti A, Altieri F, Cervoni L, Fracchiolla G, Giudici M, Guerrini U, Lavecchia A, Montanari R, Di Giovanni C, Paradiso A, Pochetti G, Simone GM, Tortorella P, Crestani M, Loiodice F (2012) Synthesis, characterization and biological evaluation of ureidofibrate-like derivatives endowed with peroxisome proliferator-activated receptor activity. J Med Chem 55:37–54

Santini C, Berger GD, Han W, Mosley R, MacNaul K, Berger J, Doebber T, Wu M, Moller DE, Tolman RL, Sahoo SP (2003) Phenylacetic acid derivatives as hPPAR agonists. Bioorg Med Chem 13:1277–1280

Spiegelman BM (1998) PPAR-γ: Adipogenic regulator and thiazolidinedione receptor. Diabetes 47:507–514

The PyMOL Molecular Graphics System, Version 1.7.4 Schrödinger, LLC.

Trott O, Olson AJ (2010) AutoDock Vina: Improving the speed and accuracy of docking with a new scoring function, efficient optimization, and multithreading. J Comput Chem 31:455–461

Waku T, Shiraki T, Oyama T, Maebara K, Nakamori R, Morikawa K (2010) The nuclear receptor PPARγ individually responds to serotonin- and fatty acid-metabolites. EMBO J 29:3395–3407

Waku T, Shiraki T, Oyama T, Morikawa K (2009) Atomic structure of mutant PPARgamma LBD complexed with 15d-PGJ2: novel modulation mechanism of PPARgamma/RXRalpha function by covalently bound ligands. FEBS Lett 583:320–324

Willson TM, Brown PJ, Sternbach DD, Henke BR (2000) The PPARs: From orphan receptors to drug discovery. J Med Chem 43:527–550

Xiao B, Su MZ, Kim EL, Hong JK, Chung HY, Kim HS, Yin J, Jung JH (2014) Synthesis of PPAR-γ activators inspired by the marine natural product, paecilocin A. Mar Drugs 12:926–939

Xiao B, Yin J, Park MH, Liu J, Li JL, Kim EL, Hong JK, Chung HY, Jung JH (2012) Design and synthesis of marine fungal phthalide derivatives as PPAR-γ agonists. Bioorg Med Chem 20:4954–4961